Technical analysis of X-ray Free Electron Lasers and the mathematical modeling and designing for optimizing their performance

Ritu Walia and Kamal Nain Chopra
Department of Physics, Maharaja Agrasen Institute of Technology, GGSIP University, New Delhi-110086, India.

E-mail: kchopra 2003 @gmail.com

(Received 2 de enero de 2019, accepted 25 de febrero de 2019)

Abstract

The mathematical Modeling and Designing of X – ray Free Electron Lasers for optimizing their Performance, based on various designing aspects, has been presented in this paper. The essential components for fabricating X-ray FEL like electron beam production system, electron beam delivery system, and electron beam utilization for emission of x-rays, have been discussed from the optimized designing point of view. The technical analysis of the radiation power, and the energy modulation of electrons in the undulator by the laser light has been done, in order to achieve laser bunching. FEL resonance condition has been discussed from the point of view of laser pulse energy, and laser pulse width. Also, Self-Amplified Spontaneous Emission FEL has been dealt with in terms of Density modulation, and Instability saturation. GINGER simulations for Noise evolution from imperfect seed have been presented from the point of view of minimizing the Noise and hence improving the quality of the laser output. The interrelationship between Numbers of longitudinal modes: $M \approx$ (bunch length)/slice, Fluctuation in the x-ray pulse energy, and the Slice properties, *i.e.* slice peak current, emittance and energy spread has been discussed for optimizing the performance of the x ray FELs. The physics phenomena affecting the e-beam like acceleration and compression, and the technical difficulties faced in this, are also explained.

Keywords: Undulator, Radiation power, Laser buncher, Magnetic field in the undulator, FEL resonance condition, GINGER simulation, Self-Amplified Spontaneous Emission FEL, and Coherent Synchrotron Radiation (CSR).

Resumen

En este documento se presentan varios aspectos del modelado matemático y del diseño de Láseres de Electrones Libres de rayos x para optimizar su rendimiento. Los componentes esenciales para la fabricación del sistema de producción, del haz de electrones tipo FEL de rayos x, del sistema de suministro del haz de electrones, y la utilización del haz de electrones para la emisión de rayos x, se han analizado desde el punto de vista del diseño optimizado. Se ha realizado el análisis técnico de la potencia de radiación y la modulación de energía de los electrones, en el ondulador, para la luz del láser, para lograr el agrupamiento del láser. La condición de resonancia FEL se ha discutido, desde el punto de vista de la energía del pulso del laser, y el ancho del pulso del láser. Además, la FEL de emisión espontánea auto amplificada se ha tratado en términos de modulación de densidad y saturación de inestabilidad. Las simulaciones de GINGER para la evolución del ruido, a partir de semillas imperfectas, se han presentado desde la perspectiva de minimizar el ruido, y por lo tanto, mejorar la calidad de la salida del láser. La interrelación entre los Números de modos longitudinales: $M \approx$ (longitud del bunch) /corte, rebanada, la fluctuación en la energía del pulso de rayos x, y las propiedades de corte, es decir, la corriente máxima de corte, la emisión y la distribución de energía, se han analizado, para optimizar el rendimiento de la x ray FELs. También se explican los fenómenos físicos que afectan al haz electrónico, como la aceleración y la compresión, así como las dificultades técnicas que se presentan.

Palabras clave: Ondulador, potencia de radiación, agrupador láser, campo magnético en el ondulador, condición de resonancia FEL, simulación GINGER, FEL de emisión espontánea autoamplificada y Radiación Sincrotrón Coherente (CSR).

PACS: 41.60.Cr **ISSN 1870-9095**

I. INTRODUCTION

The free-electron laser (FEL) had been developed at Stanford, by John Madey and his collaborators in the 1970s.

As we know, it is based on a complex combination of Particle-accelerator and Laser Science and Technology. In general, FELs have been developed at IR or Near UV wavelengths. The advancement of experimental and technological has made it possible, to develop X-ray free-electron lasers. They have in fact, revolutionized the studies of matter at the atomic and molecular level, including taking of atomic resolution snapshots on the ultrafast timescale, as in case of the intrinsic atomic motions of atoms in matter,

which was not possible, by using photons for the investigation of matter, *e. g*. sunlight and the laser.

Some of the novel exciting experiments by using the X-ray free-electron laserareL Creation of matter from the vacuum, by taking an atomic scale motion picture, of a chemical process in a time of a few femtosecond; or knowing and understanding the complex molecular structure, of a single protein or virus.

Recently, researchers have shown great interest in the design and development of unconventional lasers [1, 2, 3, 4].

During the last decade or so, many researchers [5, 6, 7, 8, 9, 10, 11, 12, 13, 14] have shown interest in investigating the Free Electron Lasers, and X-ray free-electron lasers.

Chopra [13, 14] has studied Free Electron Lasers, and X-ray free-electron lasers, with special emphasis on the unconventional modes in lasers, with spatially varying gain and loss. In this paper, we have extended this study [14], by presenting the Mathematical Modeling and Designing for optimizing their Performance.

The X-ray FEL essentials are: Electron beam production system, Electron beam delivery system, and Electron beam utilization for emission of x-rays. The main important component of such lasers are: Undulator, Electron beam, and Laser, the last one is not required in certain cases. The undulator is as shown below:

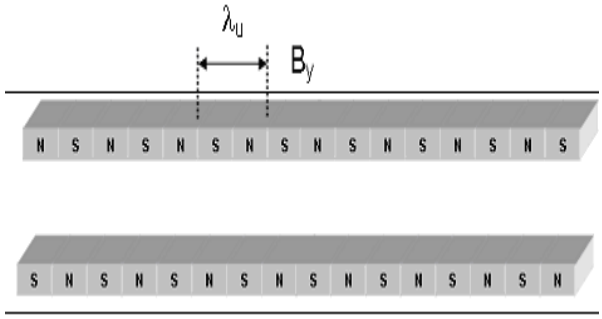

FIGURE 1. Schematic of undulator, λ_u is the undulator wavelengthm and B_y is the peak magnetic component in y direction.

Magnetic field in the undulator can be expressed by the following figure:

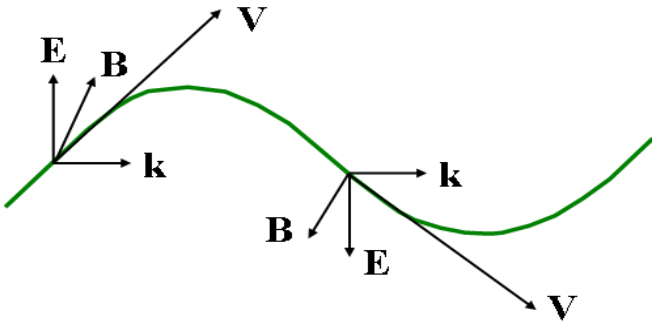

FIGURE 2. Magnetic field in the undulator. *E*, *B*, *k*, and *v* denote electric vector, magnetic vector, propagation vector, and velocity of the wave.

II ELECTRON TRAJECTORY THROUGH UNDULATOR

It is customary to study the motion of electrons moving in an undulator along the longitudinal (=*z*) axis, and describe it in the six-dimensional (6-D) phase space spanned by coordinate variables: $r_\perp$, $\beta_\perp$, γ and ψ. Where, $r_\perp$ and $\beta_\perp$ are the transverse position and relative velocity, γ is the normalized energy, and ψ is the longitudinal position. It is to be noted that while simulating the FEL process, the coordinate variables have to be obtained by solving the relevant equations at discrete longitudinal positions, according to zm= $\Delta\zeta$. Where *m* is an integer representing the step number, and $\Delta\zeta$ is the step interval, usually chosen as an integeral multiple of the undulator period λ_u .

Electron trajectory through undulator is determined by the undulator period. The laser wavelength is given by the following expression.

Laser wavelength is:

$$\lambda_w = 2\gamma^2\lambda_L/(1+K^2/2)\,. \qquad (1)$$

The variables $r_\perp$ and $\beta_\perp$ are obtained by solving the equation of motion of electrons, moving in the magnetic field of the undulator, and for the analysis and designing, is decomposed into three terms namely: betatron oscillation, fast wiggling motion and trajectory wander. The term betatron oscillation results from the focusing magnets, and is computed by using the transfer matrix, representing the lattice function of the undulator beam line. The fast wiggling motion and the trajectory wander result from the undulator field, including errors and are computed, after knowing the undulator field distribution. As can be easily observed that the fast wiggling motion just vanishes, when averaged over the electron distribution, and the trajectory wander are common to all the electrons, after normalization.

The longitudinal position ψ satisfies the following equation:

$$\frac{d\Psi}{dz} = \frac{2\pi}{\lambda_u} + \frac{\omega_f}{c}\left(1 - \frac{1}{\beta_\perp}\right)\,. \qquad (2)$$

Where c is the speed of light and ω_f is the fundamental frequency of undulator radiation emitted from a reference electron, with the average energy of $\hbar\omega$. Note that: ψ denotes the position relative to the reference electron, in units of angle, and thus, is usually referred to as the electron phase.

The remaining variable γ is given, by solving the equation describing the energy gain or loss, of each electron moving along the undulator axis, and interacting with radiation. In order to solve this energy equation, we first expand the electric field of radiation, into a Fourier series with the fundamental frequency of, namely:

$$E(\mathbf{r}_\perp, z, t) + \sum_{n=1}^{\infty} E_R^*(\mathbf{r}_\perp, z, t) \exp[in\omega_f(z/c - t)] + c_* c_{**}. \quad (3)$$

Where? is the complex amplitude of the *n*th harmonic radiation, and is supposed to be a slowly varying function of *z* and *t*.

Electron beam conditioning provides correlation of electron transverse amplitudes with electron energies to prevent de-bunching of electrons, as shown below:

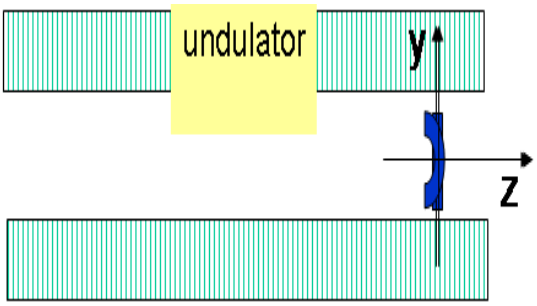

FIGURE 3. Electron beam conditioning. Figure courtesy Sessler, Whittum and Yu.

(i) Microbunching *i. e.* electrons and Waves traveling together

We consider that at a certain time the B-field of the already existing wave and the electron transverse velocity *v*T create a Lorentz force pushing the electron towards a wave node, which in fact leads to microbunching. Also, it has to be understood that the speed difference (c−u) between waves and electrons makes microbunching possible.

If this is not the case, and the electron and wave travel together with exactly the same speed, then after one-half of the undulator period, the electron transverse velocity would be reversed , but the wave *B*-field would continue in the same direction; which would lead to the reversal of the Lorentz force, and hence there will not be any microbunching.

However, this does not happen so since the electron and the wave do not travel with the same velocity.

Thus, we see that (u−c) difference is actually responsible for creating the conditions for the continuation of the microbunching.

Laser bunching takes place as a result of the Energy modulation of electrons in the undulator, by the laser light is shown in Figure 4.

The performance of the laser system depends on various undulatop parameters. Following the approach of Phillips, undulator parameters and the related equations can be obtained. The equations for the electric field, for single and multiple electrons can be expressed as:

$$E(\omega)_{\text{single-electron}} = E_0(\omega) e^{i(\omega-\omega_0)t}, \quad (4)$$

$$E(\omega)_{N-electrons} = E_0(\omega) \sum_j^N e^{i(\omega-\omega_0)t_j}. \quad (5)$$

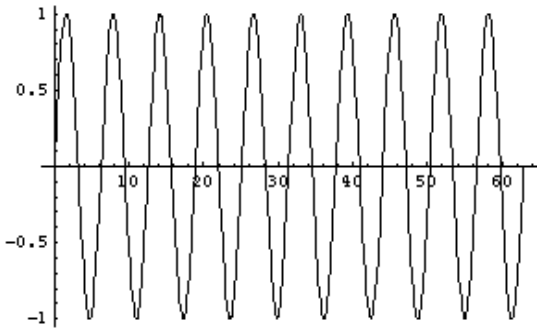

FIGURE 4. Laser bunching.

The corresponding equations for the Radiation power can also be expressed as:

$$W_{\text{N-electrons}} = W_{\text{single-electron}} \left| \sum_{j=1}^{N} e^{i(w - w_0)t_j} \right|^2, \quad (6)$$

$$= W_{\text{single-electron}} \left[N + N(N-1) e^{-\frac{1}{2}(\lambda - \Lambda x)^2} \right], \quad (7)$$

Electrons should stay bunched within:

$$\Delta z \approx \frac{1}{k} = \frac{\lambda_x}{2\pi}. \quad (8)$$

III FEL RESONANCE CONDITION

It has to be understood from the theory of FEL, that while propagating one undulator period, the electron is delayed with respect to the light on one optical wavelength.

Also, it is known that the Laser pulse energy interacts with the Spontaneous emission energy to according to the following equation:

$$A = A_L + A_R + 2\sqrt{A_L A_R \Lambda\omega_L / \Lambda\omega_R} \cos(\varphi), \quad (9)$$

where A denotes the total energy, A_L the Laser pulse energy, A_R the Spontaneous emission energy, φ the phase

difference between the two, and $\Lambda\omega_R$ and $\Lambda\omega_L$ the frequency spread of the Laser pulse energy and the Spontaneous emission energy respectively. The designer has to ensure that $\Lambda\omega_R$ has to be more or at least equal to $\Lambda\omega_L$, since the interaction takes place only under the condition:

$$\Lambda\omega_R \geq \Lambda\omega_L .$$

Also the Laser pulse width can be represented as shown below:

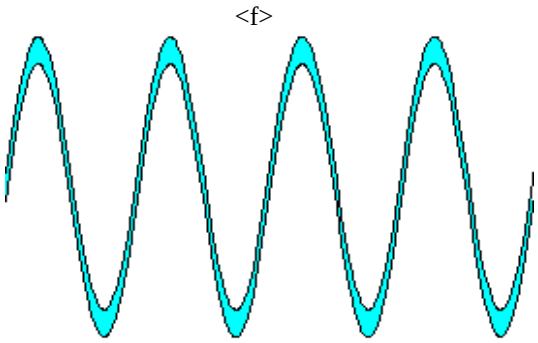

FIGURE 5. The Laser pulse width. *f* is the electron phase relative to the laser wave at the undulator entrance.

The computations of the dependence of energy on phase for the existing phase space, and for the phase space entering the radiator, can be done for the particular geometry under consideration, and for certain values, as reported in the literature have been reproduced in Figure 6.

It can be seen that though the shape of the spread remains qualitatively similar, the quantitative difference is quite marked, especially w. r. t. the phase, which increases about 4 times. This can be explained, on the basis of the noise that enters during the entrance in the radiator. It has to be appreciated that these Power *vs*. *z* and g-q scatter plots, have also been obtained experimentally by various researchers in different laboratories. Though the shapes are slightly different from each other, yet they are qualitatively similar, and show that the simulations and experimental, for the purpose of showing that the curves are quite matching, some of them have been reproduced in the Figure 7.

It can be observed clearly that at each modulator, the radiation interacts with "fresh" e- field, which in turn leads to phase multiplication, at each harmonic upshift (modulator to radiator), macro-particle by *n*. Also, the bunching effects of dispersive section visible in change from Z=6 m in 48-nm modulator, to *Z=0*.4 m scatter plot in 12-nm radiator, which is qualitatively observed from the simulations and computations.

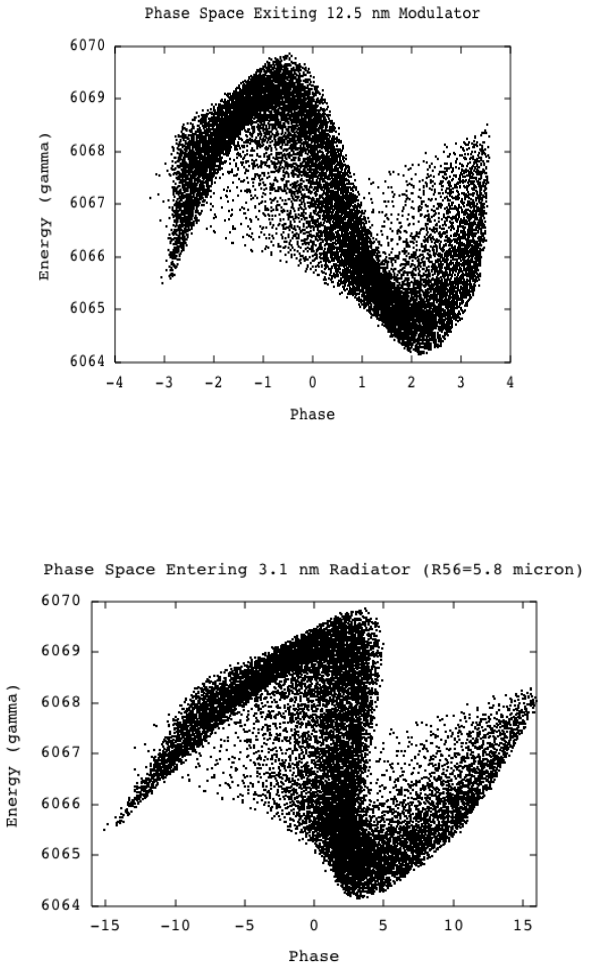

FIGURE 6. The dependence of energy on phase for the existing phase space (top), and for the phase space entering the radiator (bottom).

Another important point to be considered is Coherent Synchrotron Radiation (CSR). The powerful radiation generates energy spread, and energy spread breaks achromatic. This leads to bend-plane emittance growth *i. e.* short bunching.

In addition, Longitudinal space charge, CSR and microbunching instability have to be studied, and based on the feedback of these parameters, the designer has to refine the design.

The process is that the initial density modulation leads to the induction of energy modulation, through longitudinal space charge forces, and then, finally converted to more density modulation by a compressor, as shown in Figure 8:
final conversion to more density modulation by a compressor, in 3 stages.
It can be observed that the Compression: Energy pulse is compressed, and also the saturation due to overmodulation, stops the growth, as shown in stage (3), which implies that gain = 10 takes place.

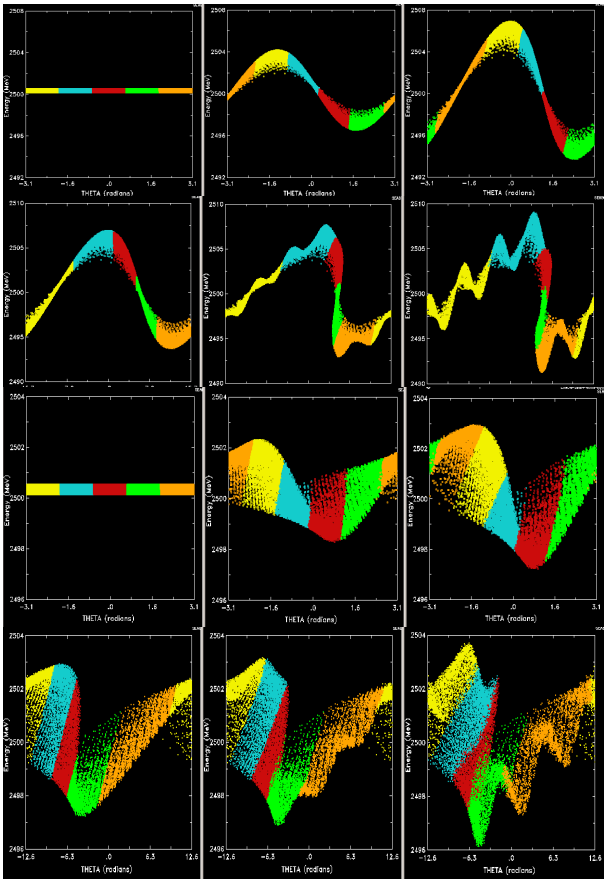

FIGURE 7. Power vs. *z and* g-q scatter plots. Figure courtesy GINGER simulations Fawley W. LBNL.

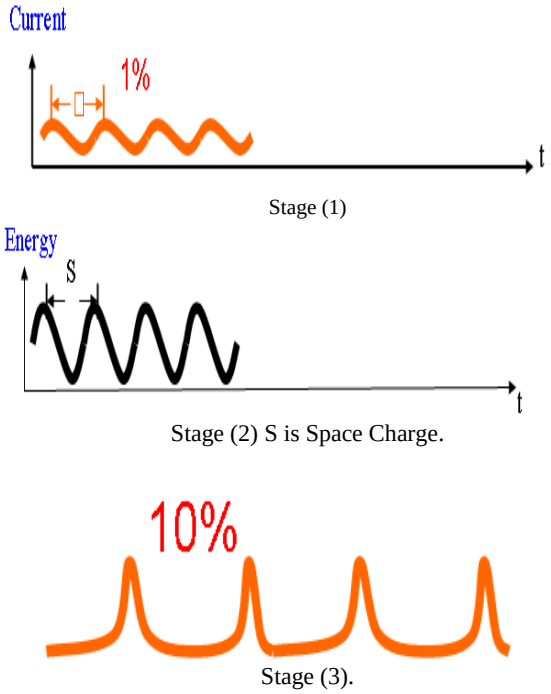

FIGURE 8. Induction of energy modulation by initial density modulation, obtained through longitudinal space charge forces.

It has to be appreciated that the electron energy spread affects both, the amplification and the saturation. It has also be noted that, the amplification starts with the optimal electron energy, as the corresponding γ-factor determines the wavelength. Also, the point to be noted is that: as the electrons transfer energy to the wave, their own energy is reduced. Because of the fact that the wave emission is different from all electrons, the different electrons have different energies, and with an increasing energy spread. As a consequence, at a certain point, the energy spread is so large, that there is no further gain *i. e.* saturation is reached.

A Microbunching instability

Entire machine with its accelerating sections, drifts and chicanes acts as an amplifier for initial density perturbation and can be characterized by a spectral gain function (in an analogy to the FELs) .

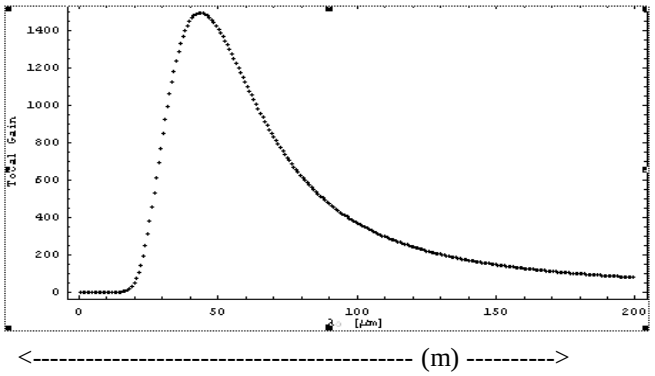

FIGURE 9. Spectral dependence of the gain of the microbunching instability. Figure courtesy Zholents. Alexander Argonne National Laboratory.

The computations show that the Instability increases rms energy spread by a factor of 5 to 10 times. This is again a parameter to be seen by the designer, and has to control the parameter so that the instability is kept within tolerable limits.

Another important point to be considered by the Designer is the harmonic multiplication of low frequency components, which results in increasing the noise. Hence, the designer of the system has to optimize and carefully choose the degree of the harmonic multiplication, so that the noise is kept to a minimum value, suitable for the system. It has to be noted that the curve in most of the cases is not equal to that done by computations, and hence correction has to be applied, by taking the feedback from the experimentally achieved data.

B. Suppression of Microbunching Instability

One of the important parameters to be taken care of by the designer is to control Microbunching Instability, which is usually done by Laser heater, an instrument for the suppression of microbunching instability. In fact, Laser heater is based on laser-e-beam interaction for inducing energy spread, by providing "Landau damping" effect

through the controlled increase of energy spread, at the beginning of the acceleration.

C Design consideration for Wakefields

It has now been well understood that: the wakefield is an electromagnetic field induced by interaction between electrons and the surrounding environment, which results in a correlated energy variation along the electron beam, and finally, results in the reduction of the FEL gain. Here, it is important to note that the designer has access to SIMPLEX, which is equipped with an option for computing the wakefield-induced energy variation, while the electron beam travels along the undulator. This helps the designer to have feedback of the performance of the X ray FEL, and thus, to make the final adjustments in the design, to achieve the optimized performance.

The designer also uses SOMPLEX for designing Slicing and parallel computing. It has to be noted that for simulating the FEL process, the whole electron beam has to be (i) divided into a number of slices with the length of slippage l along the longitudinal axis; and (ii) the bunch factor *bn* computed for all the slices at each step *zm*. This is followed by computing the radiation field amplitude at the next step *zm+1*, by taking into account the slippage effect, and also the six coordinate variables of each macroparticle.

Since the number of slices to cover the whole electron beam is quite large, leading to a considerable amount of time for completion of a single simulation, the use of SIMPLEX is quite handy. As it is equipped with a parallel-computing option, based on the message passing interface (MPI) protocol, for the purpose of reducing the computation time, in which, many numerical processes run simultaneously in parallel enabling the designer to solve the FEL equations for a number of slices at every step. It is important for the designer to control the Alignment errors and orbit distortions, which are responsible for transverse wakefields produced by e-beam, which twist e-beam into a banana shape.

In addition, other wakefields like Longitudinal wakes, Resistive wall wakes, and Surface roughness wakes, which though do not affect slices, but produce similar global variations, which adversely affect the performance of the FEL.

The designer has to take into consideration that, the CSR wake is strong at very small scales (~1 mm).

It has been observed that improvement can be obtained by using electron beam conditioning (Fig.10), which allows relaxed emittance requirement in FEL. It is quite common to use Laser-assisted electron beam conditioning for this purpose. In this case, the equations can be shown to be represented as:

$$z_2 = z_1 + \frac{1}{2}\int \left(x'^2 + y'^2 \right) \, ds \tag{10}$$

$$\delta\gamma = \Delta\gamma_1 - \Delta\gamma_2 ,$$

$$\sim k_L \left(J_x + J_y \right) \cos\left(k_L z_1 \right). \tag{11}$$

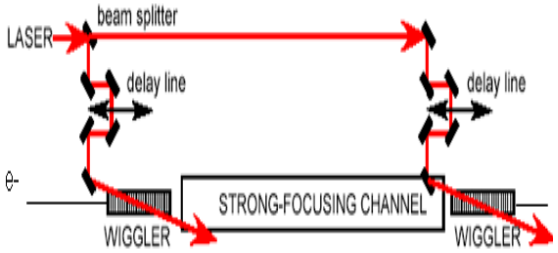

FIGURE 10. Laser-assisted electron beam conditioning Figure courtesy Zholents.Alexander Argonne National Laboratory.

It has been determined by computation, and also experimentally reported in the literature that a factor of:

$$10^5 \; to \; 10^6 .$$

in efficiency is obtained by utilizing laser and wiggler for electron energy modulation, instead of RF cavities, *i.e.*

$$k_L \; / \; k_{RF} \sim 10^5 \; to \; 10^6 .$$

This improvement can also be achieved by Enhanced Self Amplified Spontaneous Emission (SASE), as shown in Figure 11:

It is to be appreciated that as in case of the optical lasers, X-ray FEL also starts from spontaneous emission.

However, the difference is that the use of mirrors is not required.

Also, the spontaneous emission is self-amplified as shown in Figure 12.

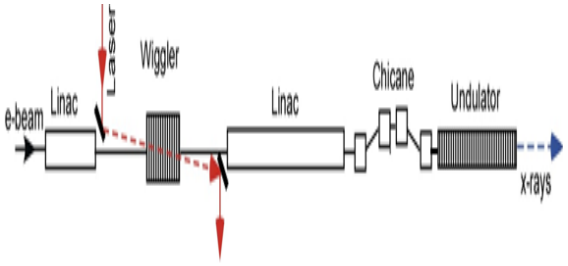

FIGURE 11. Enhanced Self Amplified Spontaneous Emission (SASE). Figure courtesy W. Fawley.

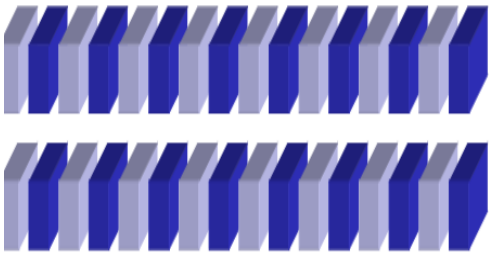

FIGURE 12. Self-Amplified Spontaneous Emission FEL.

D. Noise evolution from imperfect seed

Noise evolution from imperfect seed, can be computed by following the approach of W. Fawley, LBNL, based on GINGER simulations.

It is suitable for the laser designer, to consider the RMS phase noise df (t)/dt after removal of average component, and is done by the following expression:

$$\left(\frac{P_{\text{signal}}}{P_{\text{noise}}}\right)_{\text{out}} \approx n^{-2}\left(\frac{P_{\text{signal}}}{P_{\text{noise}}}\right)_{\text{in}} . \qquad (12)$$

So, GINGER simulation can be done by comparing the ratio of $\left(\frac{P_{\text{signal}}}{P_{\text{noise}}}\right)$ 4 at the input and the output –stage of the cascade configuration, and can be optimized for a particular value of *n*.

The value of the noise is computed for the number of harmonics from 1 to 100, and the graph is plotted for the RMS phase noise (rad/sec) *w. r. t.* harmonic *n*.

From the plot, the minimum value of noise is obtained. It can be seen from the simulations that the minimum noise is around n equal to 5-6. The curves obtained and reported in the literature for the region 240 nm $\Rightarrow$ 1 nm; have been reproduced in Figure 13.

These curves have been computed for the Input laser seed initialized with broadband, for both phase noise, and amplitude noise. It is clear that, both noise curves are similar in shape, but the one for the amplitude is lower than for the phase.

These results are easy to understand since the noise is affected in the similar manner by harmonic multiplication, though the fluctuations in phase are more random than amplitude. These results have been obtained for the case of the Fields resolved in simulation on 240 nm/c temporal resolution or better. Also, for this case, Noise reaches minimum at 48-nm, and in later stages, noise increases due to the harmonic multiplication of low frequency components.

Thus, the optimized designing is a tedious process, and some times, apart from the experience and understanding of the effect of each individual parameter, help from the commercially available software is also needed.

The results of the radiation intensity *vs*. distance are very interesting. After the start, there is an exponential growth, and then it becomes saturated. Such a case has been reported in the literature, and has been reproduced in Figure 14.

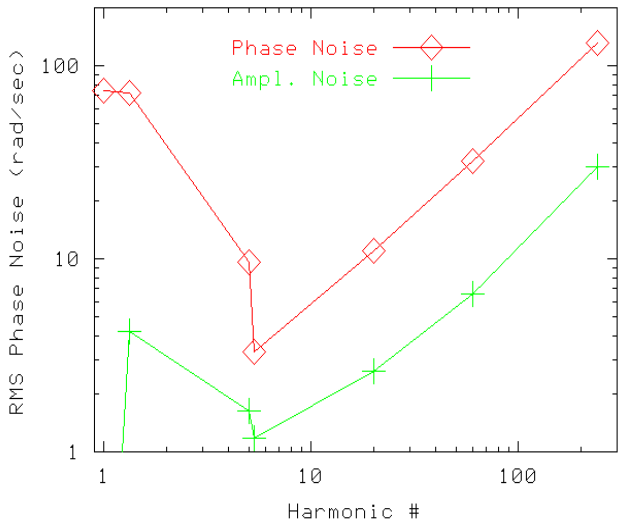

FIGURE 13. RMS phase noise (rad/sec) w.r.t. harmonic n. Figure courtesy Fawley W.

It has to be understood that the working is such that the Density modulation (shot noise at start or micro bunching latter) and the energy modulation drives each other. As is expected, the Instability reaches saturation after all electrons are micro bunched, which in fact means that the rate of de-bunching is equal to the rate of bunching. The simulations show that the bunching length is of the shape shown in Figure 15. Slice *i.e*. Cooperation length L_c , bunch length *B. L.*

Number of longitudinal modes *M*, and Fluctuation in the X-ray pulse energy are interrelated by the following expressions:

Number of longitudinal modes:

$$M \approx \frac{B.L.}{L_C} . \qquad (13)$$

$$\text{Fluctuation in the x-ray pulse energy} \sim \frac{1.}{\sqrt{M}} \qquad (14)$$

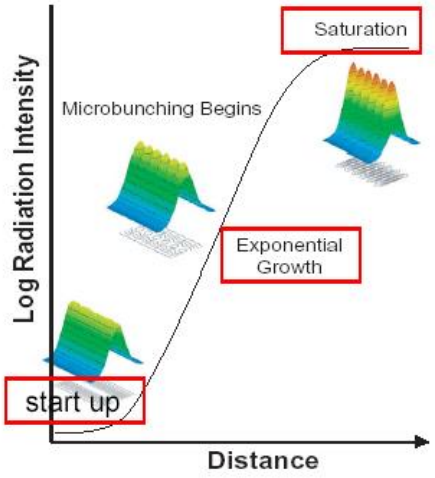

FIGURE 14. Variation of Log radiation intensitywith distance. Figure courtesy Huang Z. Stanford Linear Accelerator Center, Stanford, California 94309, USA.

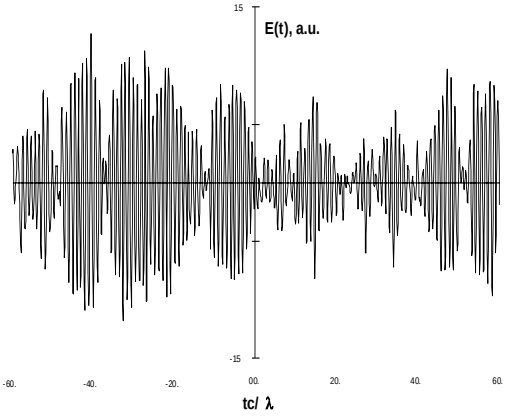

<----------(bunch length BL) ---------->

FIGURE 15. Bunching length.

The performance of the system depends on the Slice properties, meaning slice peak current, emittance, and energy spread. It has to be appreciated that the designer has to consider many parameters including Cooperation length, bunch length (*B. L.*), Number of longitudinal modes M, and Fluctuation in the X-ray pulse energy, and thus optimizing the performance of the system is a really complicated job.

Again, as pointed out above, in some cases, in addition to the experience and understanding of the effect of each individual parameter, help from the commercially available software is also needed. It has been observed both theoretically and experimentally that M decreases as coherence builds up during the exponential gain, and is able to reach a minimum level of (~150 at LCLS).at saturation.

Following the same approach, we can write the following expressions for L_C, and energy E :

$$L_C \approx \left(\frac{\lambda_x}{2\pi\rho}\right), \tag{15}$$

$$E(t) = \sum_j e^{i(\omega t - kz)}. \tag{16}$$

It has to be appreciated that the Physics phenomena affecting the e-beam while acceleration and compression are as: Non-linear effects in bunch compression of waveform, Longitudinal and transverse wakefields in accelerator, Space charge effects (mainly longitudinal), Coherent synchrotron radiation (CSR) and emittance excitation, and Resistive wall wakefields in undulators. In addition, some technical issues have to be taken care; of which are as: Jitter in the rf phase and amplitude in accelerating structures.

Intensity and timing jitters in photocathode gun laser, Misalignment of rf structures and magnetic elements, and Power supply ripples. It must be noted that, all these parameters are in some ways are related to the performance, and the designer of the laser system base to optimize the design by giving weightage to all these parameters.

IV. CONCLUDING REMARKS

It can be safely concluded that: the X-ray FELs are as good as the electron beam is. *i. e.* the peak current, slice remittances, and the slice energy spread, are the important parameters for the optimum designing of such lasers. Also, the production of a high-brightness electron beams, and preservation of the electron beam quality is affected by various factors, including: space charge, coherent synchrotron radiation, microbunching instability, and various wake fields. These have to be well understood by the designer, in order to achieve the optimized performance.

This requires great experience, intution, and patience on the part of the designer, who in some cases has to take help from the commercially available software.

It is also important to note that: the Laser-assisted manipulation of electrons in the phase space has also proved to be an important concept in the designing of the recent advanced FELs. In addition, the electron beam conditioning, and the enhanced self-amplified spontaneous emission have helped in the designing of the FELs for the improved and improvised performance.

More work is required to be done on the novel designing of the FELs, because in future laser laboratories, emphasis is on creating FEL-based multi-user X-ray facility, which will be fed by a high-repetition rate linac (up to MHz) equipped with a high brightness source of electrons. In fact, already a good amount of success has been achieved in this direction.

Optical lasers are increasingly been used for the production and shaping the electron bunches, and for seeding the x-ray radiation. It has also to be appreciated that, the advent of high-average power lasers has boosted the high-repetition rate FELs.

More research efforts are being made on the use of the FELs, for producing laser-like nearly Fourier transform limited x-ray beams, at various wavelengths with controlled pulse duration, bandwidth, and polarization. These have great applications in the research areas and medical field.

The points discussed in the present paper, can be useful for the engineers engaged in improving the performance of the X ray FELs. Huang and Kim [15] have pointed out that the high-gain free-electron lasers are being developed, as extremely bright sources for a next generation X-ray facility, and have reviewed the basic theory of the start-up, the exponential growth, and the saturation of the high-gain process, emphasizing the self-amplified spontaneous emission.

Huang and Kim [16] have also discussed the radiation characteristics of an X-ray FEL, including its transverse coherence, temporal characteristics, and harmonic content.

In addition, FEL performance in the presence of machine errors and undulator wakefields, has been examined, and various enhancement schemes through seeding and beam manipulations, have been summarized.

Here, it is important to note that very recently (16), Daresbury hosted an international workshop “Designing Future X-ray FELs", which was the first such workshop of its kind; and was attended by over 50 leading international scientists, who are engaged in creating the software using the

latest computer hardware to design and squeeze the best possible performance, from future Free Electron Lasers. The scientific and technical engineers from the CI/ASTeC and the Hartree Centre, were seriously involved at the place, where the CLARA FEL test facility was being built.

As emphasized by the Chairperson of the workshop, Brian McNeil of Strathclyde University, there was a lot of international interest in the workshop, and they managed to attract participants from as far as Stanford and Spring-8, to their EU colleagues at DESY, SwissFEL and many others.

In fact, many new ideas were discussed, and a few collaborations started, as a result of the workshop.

It is very important to appreciate the fact that now, X ray FELs have being increasingly used in a novel field of atomic-resolution imaging. Sun *et al* [17] have recently discussed that with the advent of ultrafast X-ray free-electron lasers (XFELs). It has been noticed that, we now have the possibility of the atomic-resolution imaging of reproducible objects (such as viruses, nanoparticles, single molecules, clusters, and perhaps biological cells), achieving a resolution for single particle imaging better than a few tens of nanometers.

It has been emphasized that improving upon this is a significant challenge, which in fact, has been the focus of a global single particle imaging (SPI), initiative launched in December 2014, at the Linac Coherent Light Source (LCLS), SLAC National Accelerator Laboratory, USA.

There, a roadmap was outlined, and significant multi-disciplinary effort has since been devoted, to work on the technical challenges of SPI (such as radiation damage, beam characterization, beam line instrumentation and optics, sample preparation and delivery and algorithm development), at multiple institutions involved in the SPI initiative.

It has also been noticed that, at present, the SPI initiative has achieved 3D imaging of rice dwarf virus (RDV), and coliphage PR772 viruses, at ~10 nm resolution by using soft X-ray FEL pulses, at the Atomic Molecular and Optical (AMO) instrument of LCLS. In addition, diffraction patterns with signal above noise upto the corner of the detector, with a resolution of ~6 Ångström (Å) were also recorded with hard X-rays, at the Coherent X-ray Imaging (CXI) instrument, also at LCLS.

It has been pointed out that (i) achieving atomic resolution is truly a grand challenge, and there is still a long way to go, in view of the recent developments in electron microscopy; and (ii) the potential for studying dynamics at physiological conditions, and capturing ultrafast biological, chemical and physical processes, represents a tremendous potential application, attracting continued interest in pursuing further method development.

Freund and Van der Slot [18] have discussed that: (i) the resolution in x-ray coherent diffractive imaging applications can be improved, by increasing the number of photons in the optical pulse; and (ii) an x-ray free-electron laser (XFEL) producing pulses with terawatt (TW) peak power and about 10 femtosecond duration, can satisfy this requirement. They have considered the conditions necessary for achieving powers in excess of 1 TW, in a 1.5 Å FEL.

In addition, by applying the MINERVA simulation code, they have conducted an extensive steady-state analysis, by using a variety of undulator and focusing configurations; in particular, strong focusing using FODO lattices, has been compared, with the natural weak focusing inherent in helical undulators. As reported by them, it has been found that the most important requirement to reach TW powers is extreme transverse compression of the electron beam in a strong FODO lattice in conjunction with a tapered undulator.

It has been found that, when the current density reaches extremely high levels, the characteristic growth length in the tapered undulator, becomes shorter than the Rayleigh range, giving rise to optical guiding. It has also been shown that planar undulators can reach near-TW power levels.

Also, they have discussed that, preliminary time-dependent simulations, and have shown that, TW power levels can be achieved, both for self-seeding and pure self-amplified spontaneous emission. Hence, their result shows that, high-resolution, single molecule diffractive imaging may be realized using XFELs.

Thus, it can be safely concluded that, the work on improving the performance of the X ray FELs is on a firm footing. Also, research efforts are going on, to use these lasers for the high-resolution, single molecule diffractive imaging.

ACKNOWLEDGEMENTS

The authors are grateful with the Dr. Nand Kishore Garg, Chairman of Maharaja Agrasen Institute of Technology, GGSIP University in Delhi, for providing the facilities for carrying out this research work, and also for his moral support.

The authors are thankful to Dr. M. L. Goyal, Vice Chairman for encouragement.

Thanks are also due to Dr Neelam Sharma, Director, and Dr. V. K. Jain, Deputy Director for their support during the course of the work.

Finally, thanks are also due to Prof. Dr. Ram Kishore for encouragement.

REFERENCES

[1] Chopra, K. N., *Mathematical designing and short qualitative review of unconventional lasers based on photonic crystals*, L. Am. J. Phys. E. **8**, 1-7 (2014).

[2] Chopra, K. N., *Analytical treatment of the theory and design aspects for the modeling and optimization of the efficiency of spin lasers*, Atti Fond G. Ronchi **72**, 37-47 (2017).

[3] Chopra, K. N., *A short note on Technical Analysis of Excimer Lasers, their optimization for laser corneal refractive surgery, and novel applications*, L. Am. J. Phys. E. **8**, 1-7 (2014).

[4] Chopra, K. N., *Technical analysis and overview of the microscopic lasers like metal-clad semiconductor nanolaser*

and subwavelength hybrid lasers, Atti Fond G. Ronchi **71**, 647-661 (2016).
[5] Altarelli, M., *From third-to fourth-generation light sources: Free-Electron Lasers in the UV and X-ray Range, in magnetism and synchrotron radiation*, (Springer, Berlin, 2010).
[6] Huang, Z., Kim, K. J., *Review of x-ray free-electron laser theory*, Phys. Rev. Special Topics Accel. Beams **10** 034801 (2007).
[7] Feldhaus, J., Arthur, J., Hastings, J. B., *X- ray free-electron lasers*, J. Phys. at. Mol. Opt. Phys. **38**, S799-S819 (2005).
[8] Emma, P., Akre1, R., Arthur, J., Bionta, R., Bostedt1, C., Bozek J., Brachmann, A., Bucksbaum, P., Coffee, R., Decker F.-J., Ding, Y., Dowell, D., Edstrom, S., Fisher, A., Frisch, J., Gilevich, S., Hastings, J., Hays, G., Hering, Z. Huang, Ph., Iverson, R., Loos, H., Messerschmidt, M., Miahnahri A., Moeller S., Nuhn H.-D., Pile G., Ratner D., Rzepiela J., Schultz D., Smith T., Stefan P., Tompkins, H., Turner, J., Welch, J., White, W., Wu, J., Yocky, G. and Galayda, J., *First lasing and operation of an angstrom-wavelength free-electron laser*, Nat. Photon **4**, 641-647 (2010).
[9] Margaritondo, G., *Elements of Synchrotron Light for Biology, Chemistry and Medical Research*, (Oxford University Press, New York, 2002).
[10] Shintake, T., Proceedings of the XXII Particle Accelerator Conference (PAC07), 25-29 June 2007, Albuquerque, NM, USA. IEEE Press.
[11] Schmueser, P., Dohlus, M. and Rossbach, J., *Ultraviolet and soft-X-ray Free-Electron Lasers*, (Springer, Berlin, 2008).
[12] Patterson, B. D., Abela, R., Braun, H. H., Flechsig, U., Ganter, R., Kim, Y., Kirk, E., Oppelt, A., Pedrozzi, M., Reiche, S., Rivkin, L., Schmidt, T., Shmitt, B., Strocov, V. N., Tsujino, S. and Wrulich, A. F., *Coherent science at the SwissFEL x-ray laser*, New J. Phys. **12**, 035012 (2010).
[13] Chopra, K. N., *A technical tutorial on Free Electron Lasers and short review of their recent novel applications*, L. Am. J. Phys.E. **12** (2018) 1310-1 -1310-6.
[14] Chopra K. N., *Theoretical analysis and exhaustive qualitative review of X-ray Free-Electron Lasers, with special emphasis on the unconventional modes in lasers with spatially varying gain and loss*, Atti Fond G. Ronchi **71**, 663-677 (2016).
[15] Huang, Z., Kim, K.-J: *Review of X-ray Free-Electron Laser theory*, Phys. Rev. Special Topics Accelerators and Beams **10**, 034801 (2007).
[16] ASTEC, *Designing-Future-X-ray*, Available in: https:// www.astec.stfc.ac.uk/Pages/Designing-Future-X-ray.
(Copies of the talks can found at the workshop website www.xrayfels.co.uk**)**.
[17] Sun Zhibin , Fan Jiadong, Li Haoyuan and Jiang Huaidong, *Current status of single particle imaging with X-ray Lasers*, Appl. Sci. Review **8**, 132 (2018).
[18] Freund H. P., Van der Slot P. J. M., *Studies of a terawatt x-ray Free-Electron Laser*, New J. Phys. **20**, 073017 (2018).